

This is the accepted manuscript version of the contribution published as:

Zhang, Y., **Wang, Z.**, Li, J., Chen, Y., Yang, J., Li, Y., Qin, J., Zhang, H., Qiu, G., Wang, X. (2026):

Temperature-driven microbial dynamics and functional shifts in a pilot-scale partial nitrification/anammox reactor treating low-ammonium rare earth tailwater

J. Environ. Chem. Eng. **14** (1), art. 120740

The publisher's version is available at:

<https://doi.org/10.1016/j.jece.2025.120740>

1 **Temperature-driven microbial dynamics and functional shifts in a pilot-scale**
2 **partial nitrification/anammox reactor treating low-ammonium rare earth**
3 **tailwater**

4

5 Yu Zhang ^{a,b#}, Zhenyu Wang ^{c#}, Jiayi Li ^{a,b}, Yongxing Chen ^{a,b}, Junfeng Yang ^{a,b},
6 Yonggan Li ^{a,b}, Jiafu Qin ^{a,b}, Heng Zhang ^a, Guanglei Qiu ^a, Xiaojun Wang ^{a,b*},
7 a. School of Environment and Energy, South China University of Technology,
8 Guangzhou 510006, China
9 b. The Key Lab of Pollution Control and Ecosystem Restoration in Industry Clusters,
10 Ministry of Education, 510006, China
11 c. Department of Technical Biogeochemistry, Helmholtz Centre for Environmental
12 Research – UFZ, Permoserstraße 15, 04318, Leipzig, Germany

13 #Yu Zhang and Zhenyu Wang contributed equally to this manuscript

14

15 ***Corresponding author.** cexjwang@scut.edu.cn (X.J. Wang)

16

17

18 **Abstract:** This study fills a critical research gap by evaluating the year-round
19 performance of a pilot-scale partial nitrification/anammox (PN/A) reactor treating low-
20 ammonium rare earth tailwater under seasonal temperature fluctuations. Operated
21 without thermal insulation, the system achieved a peak total nitrogen removal
22 efficiency of 87.5% during warm periods, while experiencing a 58.4% decline in winter.
23 Microbial analyses revealed that all core functional groups were affected by cold stress.
24 Notably, the PN reactor maintained suppression of nitrite-oxidizing bacteria, preserving
25 community structure integrity, with *Nitrosomonas* maintaining 11.46% relative
26 abundance. In contrast, *Candidatus Brocadia* declined from 15.26% to 4.89%, while
27 denitrifying bacteria exhibited stronger cold tolerance and maintained nitrogen removal
28 via denitrification. Pathway and electron transport analyses confirmed a functional shift
29 from Anammox to denitrification during low-temperature periods. The findings offer
30 practical insights into improving PN/A stability under seasonal variation and provide
31 guidance for advancing its engineering application in the treatment of low-ammonium
32 wastewater.

33 **Key words:** partial nitrification/anammox; bacteria activity; metagenomic; temperature
34 shock

35

36

37

38

39 **1. Introduction**

40 Rare earth elements, often referred to as the "vitamins of modern industry," are
41 increasingly utilized in advanced materials and high-tech applications. In southern
42 China, ammonium sulfate is commonly used in the extraction of ion-adsorption rare
43 earth deposits, leading to the release of substantial ammonium into surface runoff,
44 forming low ammonia nitrogen tailwater [1]. The ammonium concentration in rare
45 earth tailwater (RET) ranges from 50-110 mg/L in spring and 90-160 mg/L in winter.
46 The uncontrolled discharge of this untreated tailwater into surface waters threatens
47 ecosystem stability and raises concerns about human exposure. The primary treatment
48 approach for RET is the modified constructed rapid infiltration system [2]. However,
49 its large land footprint, high operational costs, and inconsistent pollutant removal
50 performance limit its practical application. Therefore, developing innovative nitrogen
51 removal technologies is crucial to mitigating the environmental impact of RET.

52 Anaerobic ammonium oxidation (Anammox) is an advanced and highly efficient
53 biological nitrogen removal technology. First discovered and named by Mulder in 1995
54 [3], Anammox has since become a focal point in both microbial and engineering
55 research [4]. The metabolic pathway of Anammox has been extensively elucidated, and
56 the process has been successfully implemented in biological wastewater treatment. The
57 partial nitrification-Anammox (PN/A) process, centered around Anammox, is a cost-
58 effective and energy-efficient nitrogen removal strategy [5]. Compared to conventional
59 nitrification-denitrification (DN) processes, PN/A can reduce aeration energy
60 consumption by up to 60%, eliminate the need for external organic carbon, and generate

61 significantly less sludge [6]. In recent years, research on PN/A has predominantly
62 focused on optimizing laboratory-scale reactors, while the number of full-scale
63 implementations remains limited. To date, only around 100 full-scale PN/A systems
64 have been successfully operated worldwide, shifting research priorities toward
65 engineering applications. For high-ammonium wastewater, such as landfill leachate [7]
66 and liquid-ammonia mercerization wastewater [8], numerous successful pilot and full-
67 scale applications have been reported. However, achieving stable PN/A performance
68 under low-ammonium conditions remains challenging. Under low-ammonium
69 conditions, AOB enrichment is inherently difficult, whereas nitrite-oxidizing bacteria
70 (NOB) can thrive in low-substrate environments, leading to process instability[9].
71 Previous studies have demonstrated that zeolite can enhance local ammonium
72 concentrations via ion exchange, suppressing excessive NOB proliferation and
73 overcoming a critical bottleneck in PN/A [10-14]. Nevertheless, the long-term
74 reliability of zeolite as a stable PN medium in low-ammonium wastewater requires
75 further experimental and engineering validation. Additionally, at low ammonium
76 concentrations and nitrogen loading rates, AnAOB exhibits slow growth, and improper
77 operational control may lead to granule deterioration, ultimately compromising process
78 performance [15]. Thus, despite its potential, the application of PN/A for low-
79 ammonium wastewater treatment still faces significant technical hurdles, necessitating
80 further investigation and optimization.

81 In the promotion and engineering application of the PN/A process, the impact of
82 seasonal temperature variations cannot be overlooked. Due to the influence of

83 temperate climates, wastewater treatment systems often experience significant
84 temperature fluctuations, which pose an additional challenge to the stable operation of
85 PN/A [16]. Previous studies have shown that within a moderate temperature range (30-
86 40°C), AnAOB and AOB exhibit high activity [17]. However, seasonal temperature
87 variations can substantially affect process performance [18]. In particular, at
88 temperatures below 20°C, the growth rate of NOB surpasses that of AOB, making it
89 difficult to maintain a stable supply of nitrite as a substrate for AnAOB [19].
90 Furthermore, low temperatures inhibit the activity and growth rate of AnAOB, thereby
91 weakening nitrogen removal efficiency [20, 21]. Studies have reported that for every
92 5°C decrease in temperature, the growth rate of AnAOB declines by 30%-40% [22],
93 consequently limiting nitrogen removal performance and negatively impacting enzyme
94 activity, reaction activation energy, and microbial growth. During winter, the activity
95 of functional microorganisms is significantly suppressed, leading to a notable reduction
96 in nitrogen removal efficiency. Although maintaining temperatures above 30°C in full-
97 scale applications can help stabilize PN/A performance, this approach incurs substantial
98 energy consumption, undermining the economic viability and sustainability of the
99 process [23]. Therefore, future research should focus on evaluating the stability and
100 engineering feasibility of PN/A under seasonal temperature fluctuations, assessing its
101 performance under natural temperature conditions. Such investigations will facilitate
102 process optimization and contribute to the broader implementation and scaling up of
103 PN/A technology.

104 In this study, a pilot-scale PN/A reactor was constructed and operated over the

105 long term to investigate its performance and microbial community dynamics under
106 natural conditions. The objectives of this study are as follows: (1) to evaluate the
107 performance and nitrogen removal pathways of the PN/A process during long-term
108 operation; (2) to assess in situ changes in the activity of functional microorganisms and
109 nitrogen removal mechanisms;(3) to explore the shifts and interactions within the
110 microbial community in response to seasonal temperature variations;(4) to elucidate the
111 impact of low temperatures on the abundance of microbial functional genes. The
112 findings of this study are expected to provide further insights into the long-term
113 operational mechanisms of PN/A and offer valuable guidance for its engineering-scale
114 implementation.

115 **2. Material and methods**

116 **2.1 The pilot-scale PN/A process**

117 The pilot-scale PN/A system was located in a rare earth mining area in southern
118 Jiangxi Province, China (24°54'16.8"N, 114°47'59.2"E). The system primarily
119 consisted of a two-stage PN reactor and an anammox reactor (Fig. 1). The PN reactor
120 was a steel cylindrical tank with an inner diameter of 3 m and a height of 4.5 m,
121 providing a working volume of 30 m³. It was packed with 80-mesh zeolite, which had
122 an ammonium adsorption capacity of 3.0 mg NH₄⁺-N/g, with a total packing volume of
123 5 m³. The reactor was aerated using a connected air blower. Similarly, the anammox
124 reactor was a steel cylindrical tank with the same working volume of 30 m³. It was
125 inoculated with a small amount of mature anammox sludge and operated using a
126 suspended sludge system rather than a biofilm-based process for nitrogen removal. The

127 treated effluent was discharged through a sedimentation tank, where hydraulic flow
128 facilitated sludge recirculation back to the anammox reactor. Both reactors were
129 equipped with online pH monitoring, liquid level sensors, and temperature control
130 instruments. Alkalinity (NaHCO_3) required for the PN reactor was supplied via a
131 metering pump from an alkalinity storage tank. The anammox reactor received carbon
132 supplementation (sodium acetate) through a metering pump from a carbon source tank
133 to maintain a suitable microbial environment and maintain a C/N ratio of 3.

134 The PN/A process was operated for one year, with the operational periods of the
135 PN reactor categorized by season as follows: cycles 1-21 corresponded to spring, cycles
136 22-72 to summer, cycles 73-134 to autumn, and cycles 135-195 to winter. The
137 anammox reactor was initiated only after the PN reactor had been successfully started
138 and stabilized to ensure the effective accumulation and conversion of nitrite within the
139 system. Subsequently, the PN/A process was operated in a two-stage sequential mode.
140 However, due to the relatively high nitrite concentration in the PN reactor effluent,
141 potential inhibition of AnAOB could occur. To mitigate this, the effluent from the PN
142 reactor was mixed with raw influent from the equalization tank before entering the
143 anammox reactor, thereby reducing nitrite concentrations and optimizing the reaction
144 conditions. The operational period of the anammox reactor was also classified by
145 season: cycles 1-30 corresponded to summer, cycles 31-91 to autumn, and cycles 92-
146 153 to winter.

147 **2.2 Wastewater and seed sludge**

148 The low-ammonium RET in this study was sourced from mining activities at a

149 rare earth mine in Ganzhou City, Jiangxi Province. The seed sludge for the PN reactor
150 was obtained from the activated sludge of a wastewater treatment plant in Longnan,
151 Ganzhou City, with mixed liquor volatile suspended solids (MLVSS) of approximately
152 3 g/L. The anammox seed sludge was collected from the Canon reactor in the laboratory,
153 with MLVSS of approximately 0.3 g/L. The specific characteristics of the wastewater
154 as shown in Tab. S1-S3 (Supplementary Materials). Other necessary elements were
155 supplied according to the literature.

156 **2.3 Analytical methods and calculations**

157 The concentrations of nitrogen species and COD were detected according to the
158 standard analysis method, all samples were filtered through 0.45 μm filter membrane
159 before analysis. The temperature and dissolved oxygen (DO) were both measured by a
160 digital DO meter (HQ30d, HACH, USA) and pH by a pH meter (PHS-3C, INESA
161 Scientific Instrument Co. Ltd, China). Mixed liquor suspended solids (MLSS) and
162 MLVSS were measured following the standard method [24]. The extraction and
163 analysis of extracellular polymeric substances (EPS) was conducted according to the
164 procedures outlined by Li [25], pre-treatment had removed any residual substances. The
165 nitrite accumulation rate (NAR), nitrogen production rate (NPR), nitrogen loading rate
166 (NLR), nitrogen removal rate (NRR), total nitrogen removal rate (TNRE), and free
167 ammonia (FA) concentration were calculated using calculation method in Text S3
168 (Supplementary Materials).

169 **2.4 PN/A functional bacterial activity**

170 A series of ex situ batch tests were conducted to evaluate the specific activity of

171 ammonium-oxidizing bacteria (SAOA) and the specific anammox activity (SAA). The
172 SAOA and SAA methods are described in Text S1-S2 (Supplementary Materials).

173 **2.5 microbiological analysis**

174 To investigate the differences in functional bacteria and microbial community in
175 the PN/A system, high-throughput sequencing was employed to analyze the microbial
176 community structure and changes in biofilm samples from different operational stages
177 of the reactors. The sludge samples were collected from suspended sludge, cycle 0,
178 cycle 20 and cycle 80 in the PN reactor. In the anammox treatment unit, the sludge
179 samples were collected on cycle 0, on cycle 50, on cycle 110. Bacterial universal
180 primers were used to amplify the 16S rRNA of the sludge sample. The analysis method
181 is described in Text S4 (Supplementary Materials). Metagenomic was extracted from
182 Anammox sludge samples for metagenomic analysis. For specific methods, see Table
183 S5 (Supplementary Materials). The raw sequencing data generated in this study have
184 been deposited in the NCBI database under accession number PRJNA1293347.

185 **3. Results and discussion**

186 **3.1. Long term performance of the PN/A reactor**

187 **3.1.1 Impact of seasonal temperature on the stable supply of nitrite**

188 Unlike conventional NOB inhibition strategies (e.g., intermittent aeration, high-
189 temperature control, and low DO), this study employed zeolite as a filler in the PN
190 reactor to facilitate a stable partial nitrification process. Zeolite has been widely
191 reported as an effective ammonia storage medium due to its high cation exchange
192 capacity and strong selectivity for ammonium ions [10]. The underlying mechanism

193 involves in situ enrichment of FA, elevating its concentration above the NOB inhibition
194 threshold (0.1-1.0 mg/L), thereby effectively suppressing NOB growth and activity,
195 ultimately leading to selective NOB washout. The PN reactor, filled with zeolite, was
196 operated for a total of 196 cycles (Fig. 2a-c). During Phase I, the reactor temperature
197 gradually increased (17-28°C), significantly enhancing AOB activity. By cycle 5, the
198 oxidation rate of NH_4^+ -N to NO_2^- -N exceeded the formation rate of NO_3^- -N for the first
199 time, and NO_2^- -N accumulation continued to increase thereafter, indicating the
200 successful startup of partial nitrification. In comparison with the original sample,
201 biofilm development was observed in the zeolite pore structure (Fig. S1). The rapid
202 establishment of partial nitrification could be attributed to two key factors: (i) the
203 introduction of zeolite promoted localized FA accumulation, inhibiting NOB growth
204 while facilitating AOB enrichment, and (ii) the continuous temperature rise further
205 accelerated AOB growth and metabolism, enhancing ammonia oxidation efficiency.
206 During this phase, the hydraulic retention time (HRT) was reduced from 48h to 24h to
207 increase the nitrogen loading rate. However, the NAR remained stable, demonstrating
208 the effectiveness of the zeolite-based strategy in maintaining stable partial nitrification.
209 During summer (Phase II), the operating temperature of the PN reactor ranged from
210 20°C to 33°C, with an average of 26°C. Influenced by the temperate climate, the region
211 experienced high precipitation in summer, leading to significant seasonal fluctuations
212 in the temperature and nitrogen content of the real RET entering the reactor. As a result,
213 influent NH_4^+ -N and NO_3^- -N concentrations exhibited considerable variation,
214 averaging 65.28 ± 20.83 mg/L and 36.32 ± 9.77 mg/L, respectively. In contrast, the

215 effluent NO_2^- -N and NO_3^- -N concentrations reached $120.27 \pm 72.72 \text{ mg/L}$ and $57.03 \pm$
216 19.80 mg/L , respectively. Notably, NO_3^- -N accumulation was significantly lower than
217 NO_2^- -N oxidation, achieving a high NAR. This result indicates that NOB activity was
218 effectively suppressed, ensuring an adequate NO_2^- -N supply to the anammox reactor.
219 As autumn (Phase III) commenced, ambient temperatures declined substantially (13-
220 30°C). Temperature fluctuations influenced the performance of the PN reactor,
221 particularly affecting AOB activity. The effluent NO_2^- -N concentration decreased to
222 $85.49 \pm 78.12 \text{ mg/L}$, with an average NAR of approximately 85%, marking a decline
223 from the summer phase (Phase 2). Previous studies have shown that when temperatures
224 drop below 15°C , AOB growth rates decrease significantly, allowing NOB to gradually
225 regain a competitive advantage. In winter (Phase IV), temperatures continued to decline
226 ($8-16^\circ\text{C}$). Despite the low temperatures, the PN reactor maintained effective NOB
227 suppression, with an average NAR of 77.12%. This result suggests that the system
228 retained partial nitrification capability under cold conditions, although overall reactor
229 performance was negatively impacted, as evidenced by a substantial decrease in NO_2^- -
230 N accumulation ($18.86 \pm 8.03 \text{ mg/L}$). Previous studies have demonstrated that low
231 temperatures generally exert a stronger inhibitory effect on AOB than on NOB [9, 26].
232 However, the limited decline in NAR observed in this study suggests that the zeolite-
233 based strategy mitigated the adverse effects of low temperatures on PN. This could be
234 attributed to the ability of zeolite to locally enrich NH_4^+ -N via ion exchange, thereby
235 maintaining FA concentrations at levels sufficient to inhibit NOB, even under cold
236 conditions. Since the anammox process relies on a 1:1 molar ratio of NH_4^+ -N to NO_2^- .

237 N, the insufficient NO_2^- -N supply during this phase led to an imbalance in the NO_2^- -
238 N/ NH_4^+ -N ratio, thereby affecting overall PN/A nitrogen removal performance.
239 Without additional temperature control measures, the system may experience a decline
240 in nitrogen removal efficiency during winter.

241 **3.1.2 Long term operation performance of Anammox reactor**

242 The Anammox reactor served as the primary nitrogen removal unit. Following the
243 successful initiation of PN in the PN reactor, the Anammox reactor was operated in
244 series with the PN reactor, forming an efficient PN/A synergistic nitrogen removal
245 system. However, previous studies have demonstrated that AnAOB are highly sensitive
246 to environmental fluctuations, with sudden changes in dissolved oxygen (DO) levels,
247 substrate concentrations, and temperature potentially inhibiting their activity [8]. In this
248 study, the Anammox reactor was initiated in May (Fig. 2d-f). Given that the
249 experimental site is located in a temperate monsoon climate zone, summer temperatures
250 were not a limiting factor for Anammox startup. In contrast, significant rainfall runoff
251 during the rainy season led to considerable fluctuations in influent water quality,
252 particularly affecting the NO_2^- -N/ NH_4^+ -N ratio. To ensure stable AnAOB growth, two
253 key measures were implemented: (i) blending the effluent from the PN reactor with
254 RET before entering the Anammox reactor to buffer substrate concentration
255 fluctuations; and (ii) inoculating the system with mature Anammox sludge to accelerate
256 AnAOB enrichment and stabilize system operation. During Phase I, as the AnAOB
257 community gradually adapted and enriched, the TNRE of the Anammox reactor
258 continuously increased, eventually stabilizing above 50%, indicating successful reactor

259 startup and achieving the expected nitrogen removal performance. Upon completion of
260 startup, the system entered the loading enhancement phase. To improve treatment
261 capacity, the HRT was adjusted. In Phase II, reactor performance further improved,
262 with the maximum TNRE increasing to 87.5%, while the NLR and NRR reached 0.131
263 kg N/m³/d and 0.107 kg N/m³/d, respectively. Additionally, due to the strong self-
264 aggregating properties of AnAOB, a large amount of deep-red Anammox sludge was
265 observed in the reactor, further confirming the activity and efficient enrichment of
266 AnAOB. In Phase III, as winter temperatures gradually decreased, the performance of
267 the Anammox reactor was significantly affected. At this stage, the ambient temperature
268 dropped to an average of 12°C, leading to a substantial reduction in NO₂⁻-N production
269 within the PN reactor, which disrupted the NO₂⁻-N/NH₄⁺-N ratio in the Anammox
270 reactor influent. When NO₂⁻-N supply was insufficient, NH₄⁺-N could no longer be
271 removed via the Anammox pathway, resulting in a sharp decline in TNRE from a peak
272 of 86.3% to a minimum of 36.4%. Consequently, the primary nitrogen removal pathway
273 shifted from Anammox to denitrification (Fig. S2). However, due to the imbalance in
274 influent nitrogen composition, the overall nitrogen removal performance of the system
275 could not recover to the levels observed in Phase II. Further analysis indicated that
276 temperature fluctuations directly influenced the dominant nitrogen removal pathway.
277 During the warmer summer and autumn seasons, Anammox played a dominant role in
278 nitrogen removal. However, as temperatures decreased, the system's nitrogen removal
279 pathway gradually transitioned from Anammox to DN. When the temperature remained
280 below 15°C for an extended period, DN contributed more to nitrogen removal than

281 Anammox, highlighting the higher sensitivity of AnAOB to low temperatures
282 compared to denitrifying bacteria (DNB). The $\Delta\text{NO}_3^-\text{-N} / \Delta\text{TN}$ ratio further confirmed
283 the predominance of DN during winter.

284 This study monitored the long-term stability of the pilot-scale PN/A system and
285 demonstrated the feasibility of using PN/A technology for treating RET. As the first-
286 stage unit in the two-stage PN/A process, the PN reactor achieved stable partial
287 nitritation over the long term, while the Anammox reactor was only affected when
288 temperatures dropped below 12°C. Considering the local climate characteristics, the
289 reaction temperature remained above 15°C for most of the year, with a lower
290 temperature risk occurring only between November and December. The Anammox
291 reactor thus transitioned from energy-efficient autotrophic to less efficient
292 heterotrophic DN-a key trade-off in PN/A system, ensuring nitrogen removal continuity
293 even under suboptimal conditions.

294 **3.2. Sludge characteristics in the PN/A reactor**

295 Sludge samples were collected at different operational phases to evaluate reactor
296 performance through sludge characterization. MLVSS and mixed liquor suspended
297 solids (MLSS) were used to quantify the sludge biomass and its active fraction (Fig.
298 3a). By the 90th operational cycle, both MLVSS and MLSS remained at high levels,
299 with the MLVSS/MLSS ratio approaching 0.8, indicating a high proportion of active
300 biomass and sustained sludge activity in the reactor. However, after 120 cycles, a
301 temperature decline led to a decrease in the MLVSS/MLSS ratio. The activity of AOB
302 was particularly affected, and after 160 cycles, a significant reduction in sludge biomass

303 was observed, with the MLVSS/MLSS ratio dropping to 0.6. AOB activity is known to
304 be governed by enzymatic processes that are highly temperature-dependent. This shift
305 directly compromised nitrite production and overall PN reactor performance.

306 For the Anammox reactor, MLVSS and MLSS exhibited a distinct trend of initial
307 increase followed by a subsequent decline over the operational period (Fig. 3b). By the
308 110th cycle, MLSS and MLVSS had significantly increased, suggesting that as the
309 reactor stabilized after startup, gradual acclimation led to biomass accumulation,
310 improving sludge quantity and active fraction. However, prolonged exposure to
311 temperatures below 12°C resulted in a decline in active biomass due to sustained low-
312 temperature stress. The correlation between temperature fluctuations, MLVSS, MLSS,
313 and nitrogen removal efficiency highlighted temperature as a critical factor in nitrogen
314 removal capacity deterioration. Moreover, low-temperature stress destabilized EPS,
315 weakening sludge structure and promoting disintegration. When the MLVSS/MLSS
316 ratio dropped below 0.7, sludge settleability deteriorated, and floating sludge was
317 observed on-site, likely due to microbial death and sludge disintegration under
318 prolonged low-temperature conditions. These results highlight that temperature stress
319 not only reduces microbial activity but also disrupts floc integrity, further impairing
320 reactor function.

321 The mean sludge activity at different operational phases was assessed. The SAOA
322 and SAA followed trends similar to MLVSS (Fig.3d-e). As the temperature decreased
323 from 30°C to 10°C, SAOA declined from a peak of 4.54 mg N/g VSS·d to 0.91 mg N/g
324 VSS·d, representing nearly a fivefold reduction, underscoring the enzymatic and

325 membrane transport limitations experienced by AOB under cold stress. The decline in
326 SAA was even more pronounced. When the temperature dropped to 10°C, the
327 metabolic rate of AnAOB significantly decreased, demonstrating partial inactivation or
328 washout of AnAOB. Furthermore, the growth rate of AnAOB was constrained by low
329 nitrogen loading rates. During the winter dry season, reduced surface runoff led to lower
330 nitrogen concentrations in the influent, resulting in decreased NLR. The coupling of
331 low NLR with low temperature created a dual constraint-both energetic and
332 physiological-on AnAOB growth, explaining the marked drop in activity and sludge
333 biomass observed during winter.

334 EPS are microbial secretions that influence sludge physicochemical properties and
335 pollutant removal efficiency [27]. EPS synthesis is dynamically regulated in response
336 to environmental signals, particularly temperature, which modulates both microbial
337 stress responses and metabolic allocation. EPS samples were collected from the
338 Anammox reactor throughout the operational period (Fig. 3c). By the 90th cycle, total
339 EPS concentration exhibited a continuous upward trend, increasing from 22.44 mg/g
340 VSS to 69.12 mg/g VSS, indicating high microbial metabolic activity. Under warm
341 conditions, elevated metabolic rates allowed microbes to allocate more energy toward
342 protein. Protein components strengthened the bioaggregate matrix, improving
343 mechanical resilience and promoting sludge granulation. The increasing
344 protein/polysaccharide ratio suggested that EPS functioned as an adaptive tool for
345 biofilm fortification under optimal temperatures.

346 Following a temperature decline to 15°C at the 110th cycle, EPS further increased

347 to 72.67 mg/g VSS. This transient spike in EPS reflects an immediate microbial stress
348 response that trigger overproduction of EPS to insulate cells and stabilize extracellular
349 microenvironments. However, as the temperature continued to decrease, prolonged
350 low-temperature stress led to a reduction in EPS production. A relative increase in
351 polysaccharide content was observed, indicating that under environmental stress,
352 polysaccharides may play a protective role. Notably, the reduction in EPS concentration
353 lagged behind the decline in SAA, indicating that while AnAOB metabolism was
354 severely inhibited, heterotrophic populations-such as DNB-remained metabolically
355 active and continued contributing to EPS synthesis. This functional redundancy
356 suggests that EPS dynamics are governed by the collective microbial consortia, not
357 solely AnAOB. The sustained EPS presence may have helped maintain reactor structure
358 despite loss of AnAOB-driven autotrophic activity. The concurrent decline in MLVSS
359 and shift in EPS composition points to microbial lysis, particularly of sensitive AnAOB,
360 under prolonged low-temperature stress. This lysis released soluble microbial products,
361 which likely served as secondary carbon sources fueling DNB metabolism [28]. This
362 cross-feeding interaction-where lysed autotrophic cells support heterotrophic activity-
363 represents a stress-adaptive survival mechanism within the microbial consortium. This
364 is further confirmed by metagenomic data (section 3.4), which show DNB enrichment
365 during winter and support the hypothesis of temperature-driven pathway shifts from
366 Anammox to DN.

367 **3.3. Microbial community population succession**

368 To investigate the temporal evolution of microbial communities in PN and

369 anammox reactors, sludge samples were collected at multiple operational stages and
370 subjected to 16S rRNA high-throughput sequencing (Fig. 4). For the PN reactor,
371 samples were taken at cycles 0, 20, 80, 120, and 190, and designated PN1-PN5.
372 Anammox reactor samples were collected at cycles 0, 50, 110, and 150, labeled AMX1-
373 AMX4. The dominant phyla in the PN reactor included *Proteobacteria*, *Firmicutes*,
374 *Actinobacteria*, and *Chloroflexi*. The relative abundance of *Proteobacteria* increased
375 from 31.7% at startup to a peak of 66.6%, followed by a slight decline to 58.9% as
376 temperatures dropped, indicating limited sensitivity to cold stress. Given the metabolic
377 diversity within *Proteobacteria*, it is plausible that certain subgroups exhibit enhanced
378 metabolic plasticity under low-temperature stress, enabling them to rapidly adapt and
379 maintain viability. In contrast, the decline in *Firmicutes* suggests limited suitability for
380 survival in the RET matrix, likely due to insufficient organic substrates to support their
381 fermentative and acidogenic metabolism. *Actinobacteria*, primarily aerobic
382 heterotrophs involved in organic matter degradation, also exhibited sensitivity to both
383 nutrient availability and temperature fluctuations [29]. *Chloroflexi*, however, showed
384 no significant decline in relative abundance under cold conditions. Their ecological
385 competitiveness under low-temperature stress may be attributed to their K-strategy
386 growth traits and robust EPS production, which supports biofilm formation and
387 environmental resistance. Within *Proteobacteria*, AOB exhibited temperature-
388 dependent dynamics. *Nitrosomonas* increased in relative abundance during reactor
389 start-up, reaching 13.42%, and further rose to 14.23% during the autumn operational
390 phase. However, its abundance declined to 11.46% under winter conditions. Neither

391 *Nitrobacter* or *Nitrospira* were detected, indicating effective suppression of NOB, and
392 confirming that partial nitrification was maintained despite low-temperature stress.
393 Notably, other denitrifying genera were also present. *Limnobacter* and *Thermomonas*,
394 both capable of nitrate reduction, were detected, with *Thermomonas* increasing from
395 1.8% to 3.47%. This suggests the formation of aerobic–anoxic microenvironments
396 within the sludge granules. The proliferation of *Thermomonas* underscores the
397 resilience of certain denitrifiers under environmental stress [30]. Overall, the functional
398 taxonomic composition of the PN reactor remained stable, indicating that low
399 temperatures primarily affected intracellular diffusion rates and enzyme activity, rather
400 than altering community structure. This functional resilience suggests that the reactor's
401 performance could recover with the return of favorable temperatures.

402 In the anammox reactor, phylum-level composition similarly remained stable
403 throughout operation. Dominant phyla included *Patescibacteria*, *Proteobacteria*,
404 *Planctomycetes*, *Actinobacteria*, and *Chloroflexi*. The relative abundance of
405 *Patescibacteria* remained high despite temperature decline. This phylum, widely
406 distributed across diverse environments, is frequently involved in DN and may function
407 as a syntrophic partner of AnAOB, utilizing their metabolic by-products. Over time,
408 *Patescibacteria* appeared to occupy ecological niches formerly dominated by
409 *Proteobacteria*, which typically require richer nitrogen and carbon sources-conditions
410 less prevalent in RET. However, *Patescibacteria* abundance declined slightly in winter,
411 potentially due to their streamlined genomes and limited metabolic capacity under low
412 temperatures. In contrast, certain psychrophilic *Proteobacteria* subgroups exhibited

413 better cold adaptation. *Planctomycetes*, which thrive under moderate temperatures,
414 showed a substantial decline under winter conditions (from 15.69% during stable
415 operation to 5.25%), consistent with the suppression of anammox activity at
416 temperatures below 15 °C. *Actinobacteria*, known for their cold tolerance and
417 production of low-temperature-active cellulases and proteases, increased in abundance,
418 indicating metabolic resilience under cold stress. *Chloroflexi*, through the secretion of
419 hydrophobic EPS, helped maintain sludge structure and mitigated biomass washout,
420 thereby preserving anammox reactor stability [31]. At the genus level, *Candidatus*
421 *Brocadia* was the primary AnAOB. Its relative abundance rose from 1.25% at startup
422 to 15.26%, but fell to 4.89% under winter conditions. This decline likely reflects
423 reduced hydrazine dehydrogenase activity, which limited growth under low
424 temperatures. Meanwhile, *Saccharimonadales*-a genus within *Patescibacteria*-
425 maintained stable abundance (36.78–56.55%) despite cold stress [32]. Prior studies
426 suggest that *Saccharimonadales* utilize polysaccharides secreted by AnAOB as amino
427 acid sources, and in turn secrete secondary metabolites that support AnAOB growth,
428 forming a “metabolic dependency–protection” symbiotic relationship [32]. This
429 relatively novel taxon is highly resilient and may support nitrogen removal via DN
430 when anammox activity is suppressed by cold stress. Additionally, the relative
431 abundance of *Thermomonas* and *Comamonas* increased during winter. These genera
432 possess nitrate reductases with low-temperature tolerance, supporting the hypothesis
433 that nitrogen removal pathways shifted toward DN under cold conditions. Cell lysis
434 under cold stress may have released soluble organic matter, further fueling DN. Taken

435 together, phylum and genus-level analyses reveal that long-term low-temperature stress
436 impaired the activity and growth of key functional microorganisms, significantly
437 reducing the performance of the PN/A process during winter. These seasonal
438 performance losses pose serious challenges for the full-scale application of PN/A
439 technology. Addressing temperature-associated constraints is thus of critical
440 engineering significance for advancing the practical implementation of PN/A process.

441 **3.4. Temperature-driven shifts in energy and nitrogen metabolism**

442 To further elucidate the functional shifts in microbial communities within the
443 anammox reactor, metagenomic sequencing was performed on sludge samples
444 collected at four key operational time points (0, 50, 110, and 150 cycle), designated
445 AMX1 through AMX4 (Fig. 5). Functional gene annotation was conducted using
446 KEGG Orthology, and the relative abundance of each gene category was quantified. In
447 anammox, CO₂ fixation primarily occurs via the reductive acetyl-CoA pathway, with
448 the Wood–Ljungdahl route serving as the dominant metabolic pathway. Several key
449 enzymes involved in this process—including ferredoxin (Fd²⁻, EC 1.2.1.74) and two
450 NADPH-dependent enzymes (EC 1.17.1.10 and EC 1.5.1.5)—exhibited marked
451 temperature sensitivity. These enzymes showed the highest relative abundances under
452 summer conditions, but their expression levels declined significantly under low-
453 temperature stress. Notably, in the AMX4 sample, the relative abundance of these
454 enzymes decreased to 75% of that observed in AMX2, suggesting that cooler
455 temperatures may impair NADPH biosynthesis and thereby hinder carbon fixation in
456 AnAOB. In contrast, the tricarboxylic acid (TCA) cycle, a central pathway for energy

457 metabolism, showed minimal correlation with temperature fluctuations, indicating
458 resilience to cold stress. Specifically, enzymes involved in NADH production, such as
459 those catalyzing 3-hydroxypropyl-ThP metabolism (EC 2.3.1.61) and isocitrate
460 dehydrogenase (EC 1.1.1.42), did not display notable temperature-dependent trends,
461 implying that TCA-mediated electron transfer remains stable under low-temperature
462 conditions. Beyond inorganic carbon metabolism, several organic carbon pathways-
463 predominantly driven by DNB-also demonstrated temperature-specific behaviors.
464 Among these, glycolysis and the pentose phosphate pathway generated substantial
465 amounts of NADH and acetyl-CoA. While the intermediate glyceraldehyde-3-
466 phosphate showed large fluctuations across samples, the terminal product of the pentose
467 phosphate pathway, ribose-5-phosphate, remained unaffected by temperature. Its
468 abundance in AMX4 reached 130% of that in AMX2, suggesting that this pathway may
469 sustain high levels of electron transfer at low temperatures, thereby providing a
470 sufficient NADH supply to support robust DNB growth.

471 Key functional genes associated with the anammox process include *hzs* and *hdh*
472 [33]. Their initial expression levels were 3.62 and 4.90 RPKM, respectively, rising to
473 79.10 RPKM and 102.60 RPKM as the reactor matured. However, under low-
474 temperature conditions, their expression in AMX4 declined to 41.10 RPKM and 46.11
475 RPKM, respectively, highlighting the substantial inhibitory effect of cold on hydrazine
476 synthesis and oxidation, and consequently on nitrogen removal efficiency. While *hao*
477 has long been recognized for catalyzing hydroxylamine oxidation to nitrite, recent
478 studies also implicate it in nitric oxide production, underscoring its pivotal role in the

479 anammox process. At its peak in AMX2, hao expression reached 227.15 RPKM but
480 progressively declined in AMX3 and AMX4. The concurrent downregulation of hzs,
481 hdh, and hao under cold stress further confirms the high sensitivity of core anammox
482 genes to temperature fluctuations. In the DN pathway, NO_3^- -N is reduced to NO_2^- -N
483 via genes such as napA/B, nasB, and narG/H/I, then to nitric oxide by nirS/K, and
484 finally to dinitrogen gas through norB/C/Z. Among these, the expression of the
485 narG/H/I subunits remained stable across temperature regimes. Additionally, the nxr
486 gene complex (nxrA/B), which catalyzes the oxidation of NO_2^- -N to NO_3^- -N, provides
487 both reducing equivalents for autotrophic nitrifiers and compensates for electron loss
488 in AnAOB. The expression of nxrA ranged from 367.35 to 416.78 RPKM and was
489 unaffected by seasonal temperature changes, suggesting that while anammox activity
490 may decline under cold conditions, it retains the potential for recovery upon
491 temperature rebound. Further analysis of DN-related gene expression revealed only
492 modest reductions in nirK and norB/Z under low-temperature conditions, indicating a
493 greater resilience of DNB compared to AnAOB. The sustained activity of key nitrate
494 reductases also implies that DN remains functionally robust at low temperatures,
495 supporting the notion that DNB may exhibit superior adaptability and maintain
496 effective nitrate reduction under cold stress [34].

497 **3.5. Towards sustainable nitrogen removal from RET via PN/A**

498 Although the application of the PN/A process has been promoted for many years,
499 research on the treatment of RET under seasonal temperature fluctuations and low-
500 strength ammonia conditions remains scarce. In this study, a pilot-scale PN/A process

501 was investigated to assess the effects of seasonal temperature variations on process
502 performance and microbial community composition during the treatment of RET. The
503 results indicate that under the relatively high temperature conditions in summer and
504 autumn, the nitrogen removal performance steadily improved, with NLR and TNRE
505 reaching peak values of $0.131 \text{ kg N/m}^3/\text{d}$ and 87.5%, respectively. This coincided with
506 enhanced SAA and biomass enrichment, suggesting that high temperatures facilitated
507 autotrophic nitrogen removal via the canonical PN/A pathway. In contrast, under winter
508 low-temperature conditions, the short-term performance of the anammox process was
509 not significantly affected, with AnAOB exhibiting strong low-temperature adaptability.
510 However, long-term operation at low temperatures failed to achieve optimal PN/A
511 performance, posing an engineering challenge-especially when temperatures fell below
512 12°C , at which the performance was only 36.4%. Encouragingly, the PN reactor
513 consistently maintained a high NAR under cold conditions, effectively resolving the
514 challenge of NOB suppression, largely due to the sustained inhibitory effect of zeolite
515 on endogenous FA concentrations. Analysis of both process data and microbial profiles
516 revealed that the contribution to nitrogen removal in the anammox reactor was mainly
517 derived from the anammox reaction during summer, whereas in winter, DN became the
518 dominant pathway. Moreover, heterotrophic DN in the reactor not only involved the
519 reaction induced by a small addition of exogenous carbon but also likely utilized the
520 slowly biodegradable organic matter released from biomass decay and fragmentation
521 to accomplish endogenous DN-findings that are consistent with other's study [35]. To
522 ensure overall stable nitrogen removal performance during winter, this study

523 recommends replacing anammox with DN for nitrogen removal during low-
524 temperature periods, while selectively enriching and reinforcing AnAOB based on the
525 annual temperature profile. This approach aligns pathway selection with microbial
526 kinetic optima, enhancing overall resilience. Given that in Ganzhou the reaction
527 temperature remains above 15°C for most of the year and drops only in November and
528 December. The scalable application of the PN/A process can be achieved by operating
529 DN during low-temperature periods and, upon temperature recovery, by adding
530 exogenous hydrazine to selectively enrich AnAOB [35]. At the hardware level,
531 strategies such as steam-assisted heating or enhanced insulation can be implemented to
532 mitigate temperature-induced performance losses and improve nitrogen removal
533 efficiency of the PN/A process. Although low temperatures affect the activity and
534 abundance of functional bacteria, the PN/A nitrogen removal pathway remains a system
535 advantage, and overcoming the constraints imposed by temperature is of significant
536 engineering importance.

537 **4. Conclusions**

538 This study constructed a pilot-scale PN/A reactor to treat low-ammonium RET,
539 and systematically investigated the long-term effects of seasonal temperature
540 fluctuations on an uninsulated system. During warmer periods, the PN/A process
541 achieved a maximum TNRE of 87.5%. However, low temperature resulted in a 58.4%
542 reduction. All core functional microbial groups were negatively impacted by cold stress.
543 Encouragingly, the PN reactor maintained effective suppression of NOB under low
544 temperature, preserving ecological niche integrity, with Nitrosomonas retaining a

545 relative abundance of 11.46%. In contrast, *Candidatus Brocadia*-the dominant
546 Anammox bacterium-declined from a peak of 15.26% to 4.89%, whereas DNB
547 demonstrated greater cold tolerance. Analyses of both nitrogen transformation
548 pathways and electron transport further confirmed the superior low-temperature
549 adaptability of DNB compared to AnAOB. These findings suggest that PN/A can
550 enhance denitrification maintains reactor performance during low temperature periods.
551 As temperatures increased, targeted operational strategies enabled the selective
552 enrichment of AnAOB, thereby overcoming the temperature limitations that hinder the
553 broader engineering application of the PN/A process.

554

555 **Acknowledgements**

556 This research was dominantly funded by Key R&D projects of Guangzhou
557 Science and Technology Plan (2024B03J1278).

558 **Reference**

- 559 [1] Z. Deng, Y. Chen, C. Zhang, Z. Chen, Y. Li, L. Huang, Z. Wang, X. Wang,
560 Improving nitrogen removal performance from rare earth wastewater via partial
561 denitrification and anammox process with Fe(II) amendment, *J Water Process Eng.*
562 60 (2024), 105131, <https://doi.org/10.1016/j.jwpe.2024.105131>.
- 563 [2] Z. Zou, H. Yang, S. Zhang, W. Chi, X. Wang, Z. Liu, Nitrogen removal performance
564 and microbial community analysis of immobilized biological fillers in rare earth
565 mine wastewater, *Biochem. Eng. J.* 186 (2022), 108559,
566 <https://doi.org/10.1016/j.bej.2022.108559>.
- 567 [3] A. Mulder, A.A. van de Graaf, L.A. Robertson, J.G. Kuenen, Anaerobic ammonium
568 oxidation discovered in a denitrifying fluidized bed reactor, *FEMS Microbiol.*
569 *Ecol.* 16 (1995), 177-183, [https://doi.org/10.1016/0168-6496\(94\)00081-7](https://doi.org/10.1016/0168-6496(94)00081-7).
- 570 [4] W. Li, P. Lu, L. Zhang, A. Ding, X. Wang, H. Yang, D. Zhang, Long-term
571 performance of denitrifying anaerobic methane oxidation under stepwise cooling
572 and ambient temperature conditions, *Sci. Total Environ.* 713 (2020), 136739,
573 <https://doi.org/10.1016/j.scitotenv.2020.136739>.
- 574 [5] Y. Zhang, J. Deng, X. Xiao, Y.-Y. Li, J. Liu, Insights on pretreatment technologies
575 for partial nitrification/anammox processes: A critical review and future
576 perspectives, *Bioresour. Technol.* 384 (2023), 129351,
577 <https://doi.org/10.1016/j.biortech.2023.129351>.
- 578 [6] H. Chen, H. Wang, R. Chen, S. Chang, Y. Yao, C. Jiang, S. Wu, Y. Wei, G. Yu, M.
579 Yang, Y.-Y. Li, Unveiling performance stability and its recovery mechanisms of
580 one-stage partial nitritation-anammox process with airlift enhanced micro-
581 granules, *Bioresour. Technol.* 330 (2021), 124961,
582 <https://doi.org/10.1016/j.biortech.2021.124961>.
- 583 [7] X. Li, M.-y. Lu, Q.-c. Qiu, Y. Huang, B.-l. Li, Y. Yuan, Y. Yuan, The effect of
584 different denitrification and partial nitrification-Anammox coupling forms on
585 nitrogen removal from mature landfill leachate at the pilot-scale, *Bioresour.*
586 *Technol.* 297 (2020), 122430, <https://doi.org/10.1016/j.biortech.2019.122430>.

- 587 [8] Z. Chen, X. Wang, S. Zhou, J. Fan, Y. Chen, Large-scale (500 kg N/day) two-stage
588 partial nitritation/anammox (PN/A) process for liquid-ammonia mercerization
589 wastewater treatment: Rapid start-up and long-term operational performance, *J.*
590 *Environ. Manage.* 326 (2023), 116404,
591 <https://doi.org/10.1016/j.jenvman.2022.116404>.
- 592 [9] H. Wang, H. Chen, L. Chen, Y. Chen, Z. Liang, E. Yang, D. Yang, X. Dai,
593 Deciphering the effect of temperature reduction on the biofilm in partial
594 nitritation-anammox system: Insights from microbial community to metabolic
595 pathways, *J. Environ. Chem. Eng.* 11 (2023), 110022,
596 <https://doi.org/10.1016/j.jece.2023.110022>.
- 597 [10] Y. Chen, C. Zhang, Z. Chen, Z. Deng, Q. Wang, Q. Zou, J. Li, Y. Zhang, X. Wang,
598 Achieving nitrite shunt using in-situ free ammonia enriched by natural zeolite:
599 Pilot-scale mainstream anammox with flexible nitritation strategy, *Water Res.* 265
600 (2024), 122314, <https://doi.org/10.1016/j.watres.2024.122314>.
- 601 [11] H. Chen, Z. Chen, S. Zhou, Y. Chen, X. Wang, Efficient partial nitritation
602 performance of real printed circuit board tail wastewater by a zeolite biological
603 fixed bed reactor, *J. Water Process Eng.* 53 (2023), 103607,
604 <https://doi.org/10.1016/j.jwpe.2023.103607>.
- 605 [12] Z. Chen, X. Zheng, Y. Chen, X. Wang, L. Zhang, H. Chen, Nitrite accumulation
606 stability evaluation for low-strength ammonium wastewater by adsorption and
607 biological desorption of zeolite under different operational temperature, *Sci. Total*
608 *Environ.* 704 (2020), 135260, <https://doi.org/10.1016/j.scitotenv.2019.135260>.
- 609 [13] Y. Zhang, J. Li, Y. Chen, J. Yang, Z. Chen, X. Wang, Rapid start-up and stable
610 operation of pilot scale denitrification-partial nitritation/anammox process for
611 treating electroplating tail wastewater, *Bioresour. Technol.* 409 (2024), 131192,
612 <https://doi.org/10.1016/j.biortech.2024.131192>.
- 613 [14] Z. Chen, Y. Chen, X. Zheng, X. Wang, Y. Wang, J. Chen, Comparison of complete
614 nitritation–denitrification and partial nitritation–anammox for iron oxide
615 wastewater treatment, *J. Clean. Prod.* 294 (2021), 126281,
616 <https://doi.org/10.1016/j.jclepro.2021.126281>.

- 617 [15] J. Zhang, L. Jiang, L. Zhang, Y. Peng, A mini review on evaluating the contribution
618 of anammox to nitrogen removal in municipal wastewater treatment systems:
619 Current limitations and suggestions for paths forward, *J Water Process Eng.* 68
620 (2024), 106462, <https://doi.org/10.1016/j.jwpe.2024.106462>.
- 621 [16] X. Gong, B. Wang, X. Qiao, Q. Gong, X. Liu, Y. Peng, Performance of the
622 anammox process treating low-strength municipal wastewater under low
623 temperatures: Effect of undulating seasonal temperature variation, *Bioresour.*
624 *Technol.* 312 (2020), 123590, <https://doi.org/10.1016/j.biortech.2020.123590>.
- 625 [17] S. Wang, K. Ishii, H. Yu, X. Shi, B.F. Smets, A. Palomo, J. Zuo, Stable nitrogen
626 removal by anammox process after rapid temperature drops: Insights from
627 metagenomics and metaproteomics, *Bioresour. Technol.* 320 (2021), 124231,
628 <https://doi.org/10.1016/j.biortech.2020.124231>.
- 629 [18] S. Zhou, Z. Song, Z. Sun, X. Shi, Z. Zhang, The effects of undulating seasonal
630 temperature on the performance and microbial community characteristics of
631 simultaneous anammox and denitrification (SAD) process, *Bioresour. Technol.*
632 321 (2021), 124493, <https://doi.org/10.1016/j.biortech.2020.124493>.
- 633 [19] M. Muszyński-Huhajło, K. Ratkiewicz, K. Janiak, S. Miodoński, A. Jurga, R.
634 Szetela, The short- and long-term effects of cold-temperature shock on partial
635 nitritation - improved assessment methodology, *J Environ Chem Eng.* 10 (2022),
636 106995, <https://doi.org/10.1016/j.jece.2021.106995>.
- 637 [20] J. Dosta, I. Fernández, J.R. Vázquez-Padín, A. Mosquera-Corral, J.L. Campos, J.
638 Mata-Álvarez, R. Méndez, Short- and long-term effects of temperature on the
639 Anammox process, *J. Hazard. Mater.* 154 (2008), 688-693,
640 <https://doi.org/10.1016/j.jhazmat.2007.10.082>.
- 641 [21] L. Li, W. Xu, J. Ning, Y. Zhong, C. Zhang, J. Zuo, Z. Pan, Revealing the intrinsic
642 mechanisms for accelerating nitrogen removal efficiency in the Anammox reactor
643 by adding Fe(II) at low temperature, *Chin. Chem. Lett.* 35 (2024), 109243,
644 <https://doi.org/10.1016/j.cclet.2023.109243>.
- 645 [22] W. Li, J. Li, Y. Liu, R. Gao, L. Deng, C. Kao, Y. Peng, Mainstream double-
646 anammox driven by nitritation and denitrification using a one-stage step-feed

- 647 bioreactor with real municipal wastewater, *Bioresour. Technol.* 343 (2022),
648 126132, <https://doi.org/10.1016/j.biortech.2021.126132>.

649 [23] J. Ji, Y. Peng, X. Li, Q. Zhang, X. Liu, A novel partial nitrification-synchronous
650 anammox and endogenous partial denitrification (PN-SAEPD) process for
651 advanced nitrogen removal from municipal wastewater at ambient temperatures,
652 *Water Res.* 175 (2020), 115690, <https://doi.org/10.1016/j.watres.2020.115690>.

653 [24] W.G.J.A.J.o.P.H. Walter, *STANDARD METHODS FOR THE EXAMINATION*
654 *OF WATER AND WASTEWATER* (11th ed.), 51 (1961), 940-940,

655 [25] J. Li, Y. Zhang, Y. Chen, Y. Zhang, J. Yang, Z. Chen, X. Wang, Crucial role of
656 extracellular polymeric substances from anammox sludge in wastewater
657 phosphorus recovery via magnesium phosphate crystallization, *J Environ Chem*
658 *Eng.* 12 (2024), 113882, <https://doi.org/10.1016/j.jece.2024.113882>.

659 [26] T.R.V. Akaboci, F. Gich, M. Ruscalleda, M.D. Balaguer, J. Colprim, Assessment
660 of operational conditions towards mainstream partial nitritation-anammox
661 stability at moderate to low temperature: Reactor performance and bacterial
662 community, *Chem. Eng. J.* 350 (2018), 192-200,
663 <https://doi.org/10.1016/j.cej.2018.05.115>.

664 [27] V.F. Dsane, H. Jeon, Y. Choi, S. Jeong, Y. Choi, Characterization of magnetite
665 assisted anammox granules based on in-depth analysis of extracellular polymeric
666 substance (EPS), *Bioresour. Technol.* 369 (2023), 128372,
667 <https://doi.org/10.1016/j.biortech.2022.128372>.

668 [28] W. Pan, Q. Wang, T. Ren, Z. Tang, Y. Chen, H. Liu, Y. Peng, H. Yue, D. Liu,
669 Achieving advanced nitrogen removal from oxytetracycline wastewater by partial
670 nitrification-endogenous denitrification: performance, metabolic pathways,
671 microorganism community, and potential applications, *J. Environ. Manage.* 382
672 (2025), 125333, <https://doi.org/10.1016/j.jenvman.2025.125333>.

673 [29] Y. Bao, J. Dolfing, Z. Guo, J. Liu, X. Pan, X. Cui, Y. Wang, Y. Jin, L. Zhang, R.
674 Chen, X. Li, Y. Feng, Warmer summers have the potential to affect food security
675 by increasing the prevalence and activity of Actinobacteria, *Eur. J. Soil Biol.* 124
676 (2025), 103708, <https://doi.org/10.1016/j.ejsobi.2024.103708>.

- 677 [30] M. Qv, D. Dai, D. Liu, Q. Wu, C. Tang, S. Li, L. Zhu, Towards advanced nutrient
678 removal by microalgae-bacteria symbiosis system for wastewater treatment,
679 *Bioresour. Technol.* 370 (2023), 128574,
680 <https://doi.org/10.1016/j.biortech.2022.128574>.
- 681 [31] X. Wang, G. Zhang, M. Hu, D. Lu, Y. Zhang, T. Zhang, T. Ya, X. Wang, Important
682 role of Chloroflexi: Improved the cooperation of anammox community under
683 PFOS stress, *Chem. Eng. J.* 499 (2024), 155950,
684 <https://doi.org/10.1016/j.cej.2024.155950>.
- 685 [32] J. Zhang, S. Lei, X. Zhang, S. Xie, Y. Zheng, W. Yang, Z. Wang, A. Chen, J. Zhao,
686 Enhanced nitrogen and phosphorus removal by *Saccharimonadales* sp. in a
687 sequencing batch reactor, *Biochem. Eng. J.* 211 (2024), 109456,
688 <https://doi.org/10.1016/j.bej.2024.109456>.
- 689 [33] W. Ai, J. Shang, Y. Wang, P. Wang, Z. Jing, X. Gao, X. Zhang, J. Zhuang, T.
690 Huang, Constructing a robust mainstream Anammox process via cold shock
691 adaptation: Nitrogen removal performance and microbial community, *J Environ
692 Chem Eng.* 13 (2025), 119443, <https://doi.org/10.1016/j.jece.2025.119443>.
- 693 [34] X. Li, M. Tang, J. Jiang, S. Ma, S. Yao, Y. Yang, Enhanced effect and mechanism
694 of biochar on the nitrogen removal of low C/N wastewater by cold-tolerant
695 heterotrophic nitrifying-aerobic denitrifying bacterium, *J. Contam. Hydrol.* 276
696 (2026), 104708, <https://doi.org/10.1016/j.jconhyd.2025.104708>.
- 697 [35] W. Zhou, Q. Zhang, B. Wang, F. Hou, H. Pang, Y. Guo, L. Zhang, Y. Peng,
698 Temperature-based strategy for enhanced nitrogen removal in mainstream via
699 selectively strengthening anammox or denitrification, *npj Clean Water.* 8 (2025),
700 23, <https://doi.org/10.1038/s41545-025-00448-4>.

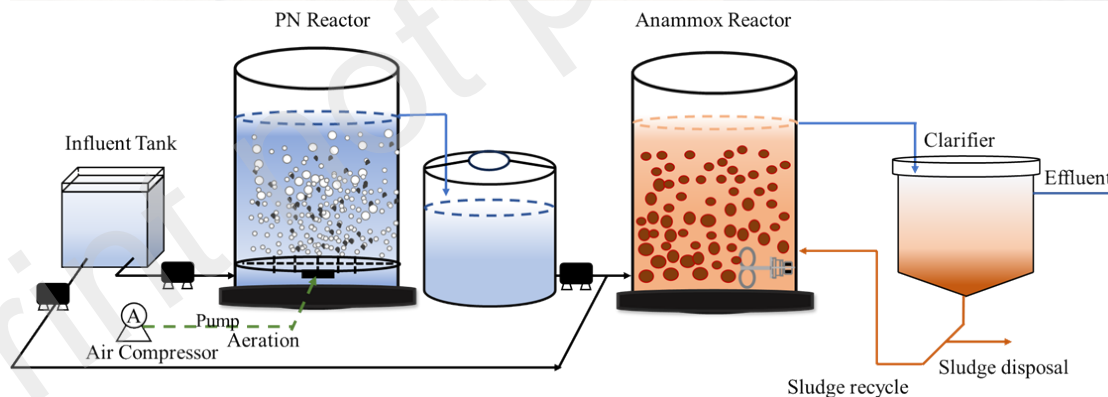


Fig. 1. Schematic of the PN/A reactor.

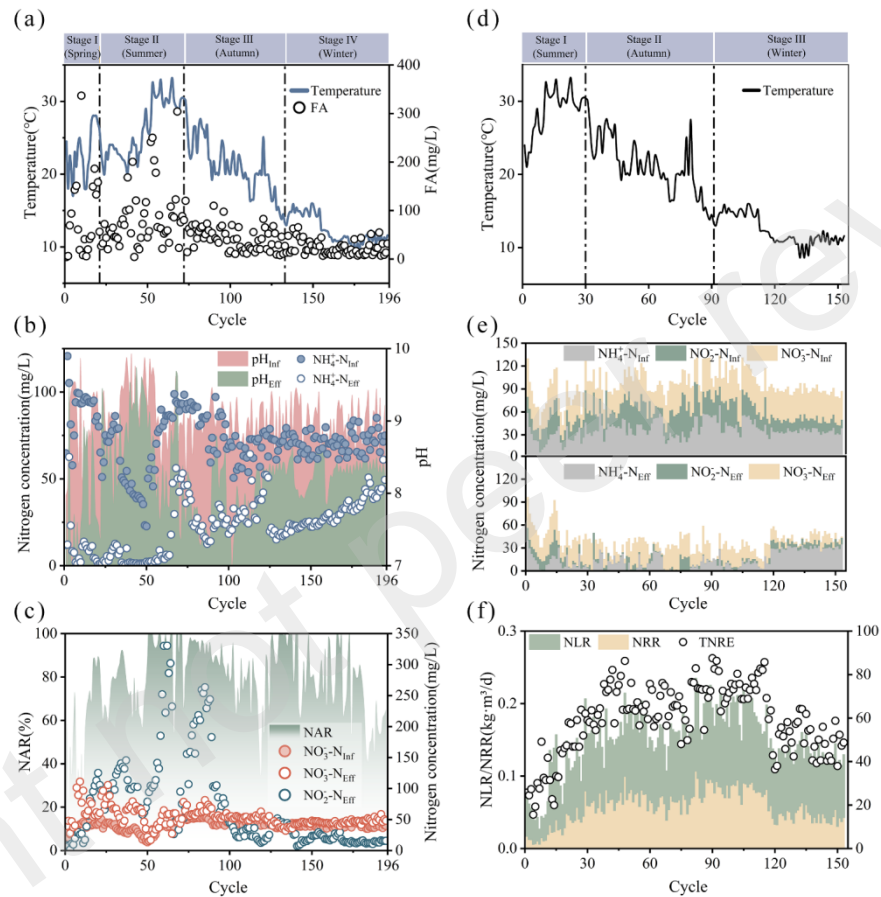


Fig. 2. Performance in the PN/A reactor: (a) FA concentration and temperature of PN reactor; (b) influent and effluent NH_4^+ -N, pH of PN reactor; (c) influent and effluent NO_3^- -N, effluent NO_2^- -N, NAR of PN reactor; (d) temperature of Anammox reactor; (e) influent and effluent nitrogen of Anammox reactor; (f) NLR、NRR and TNRE of Anammox reactor.

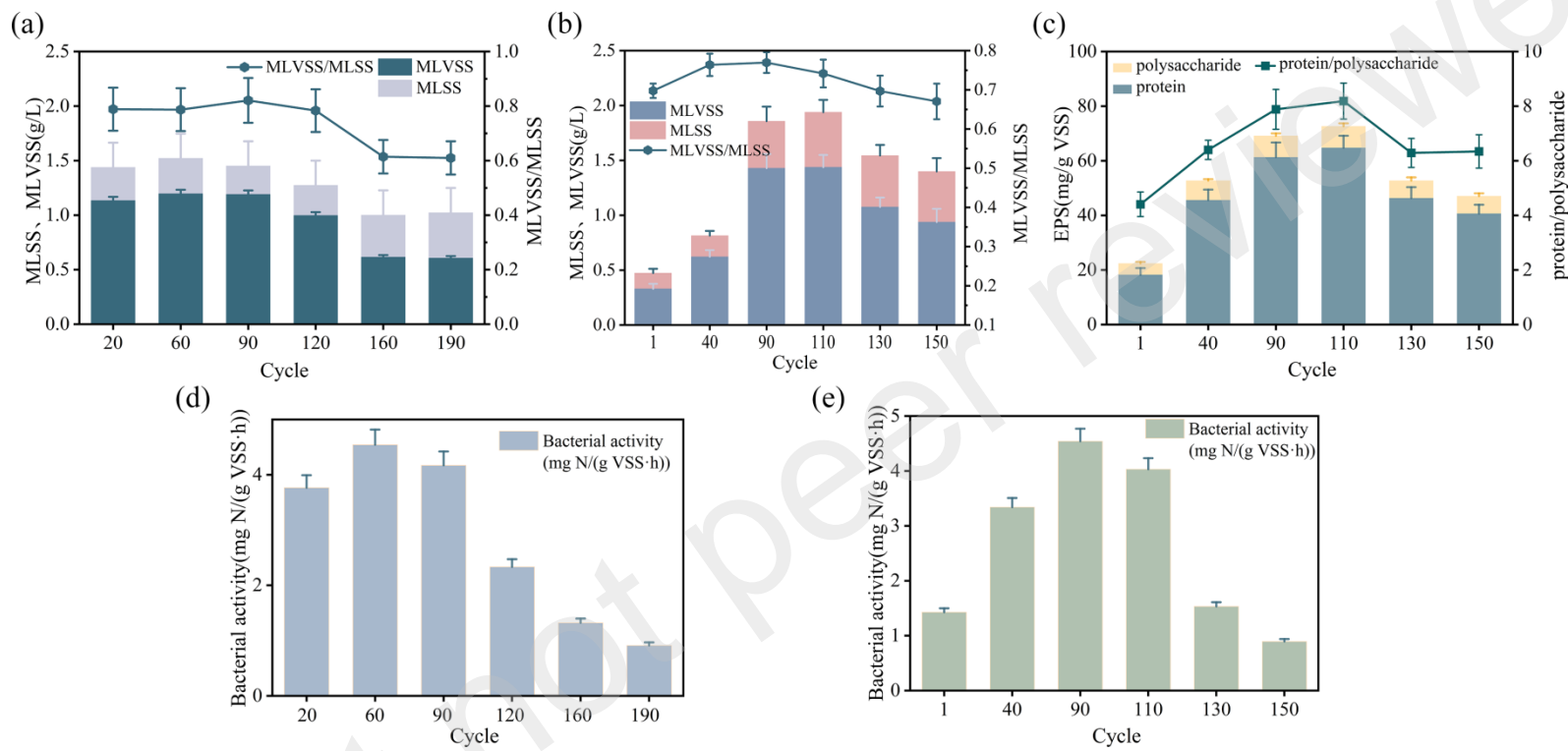


Fig. 3. Characteristics of sludge in PN/A reactor: (a) MLVSS、MLSS and MLVSS/ MLSS of PN reactor; (b) MLVSS、MLSS and MLVSS/ MLSS of Anammox reactor; (c) extracellular polymeric substance of Anammox reactor; (d) SAOA of PN reactor; (e) SAA of Anammox reactor.

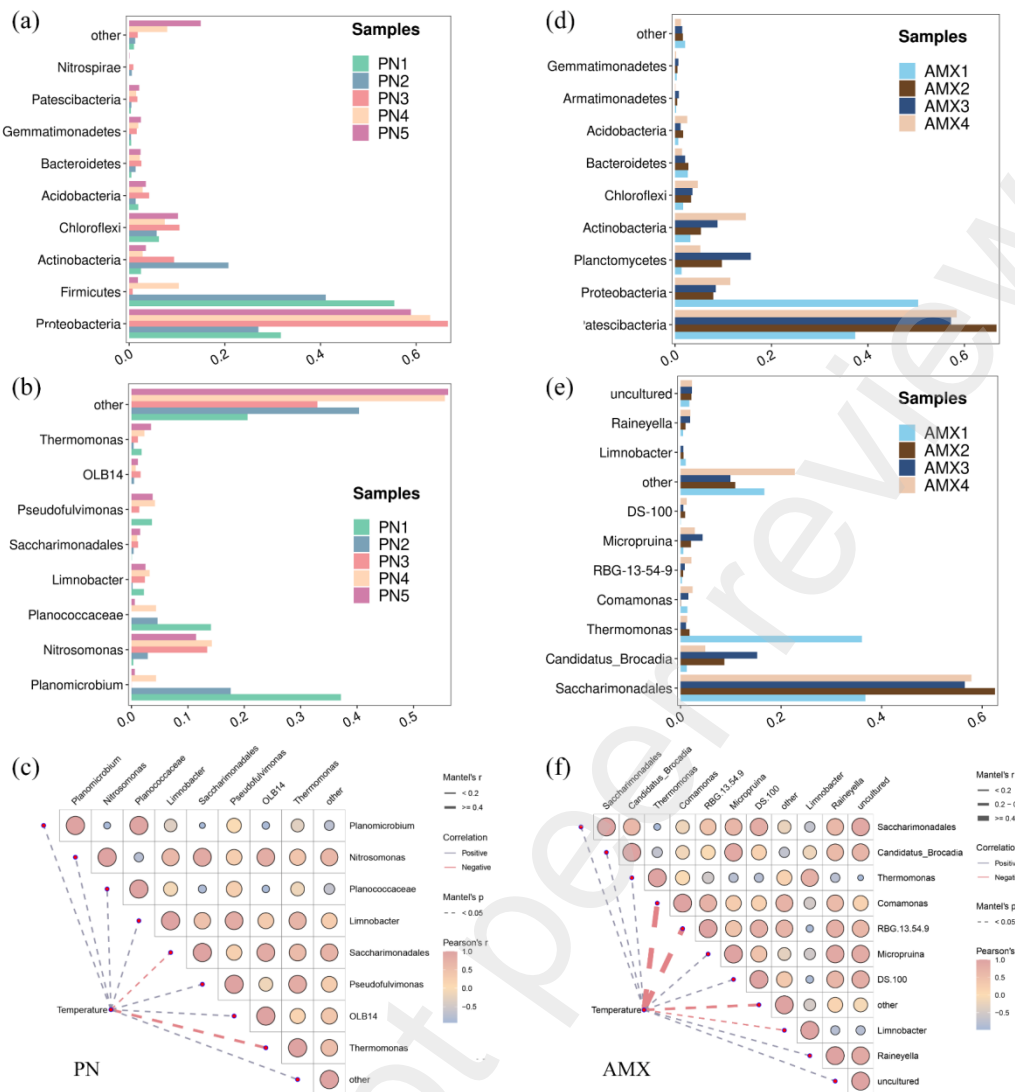


Fig. 4. Taxonomy classification of bacterial community composition of the PN/A reactor (a) phylum level in PN reactor; (b) genus level in PN reactor; (c) correlation between temperature and genus in PN reactor; (d) phylum level in Anammox reactor; (e) genus level in Anammox reactor; (f) correlation between temperature and genus in Anammox reactor.

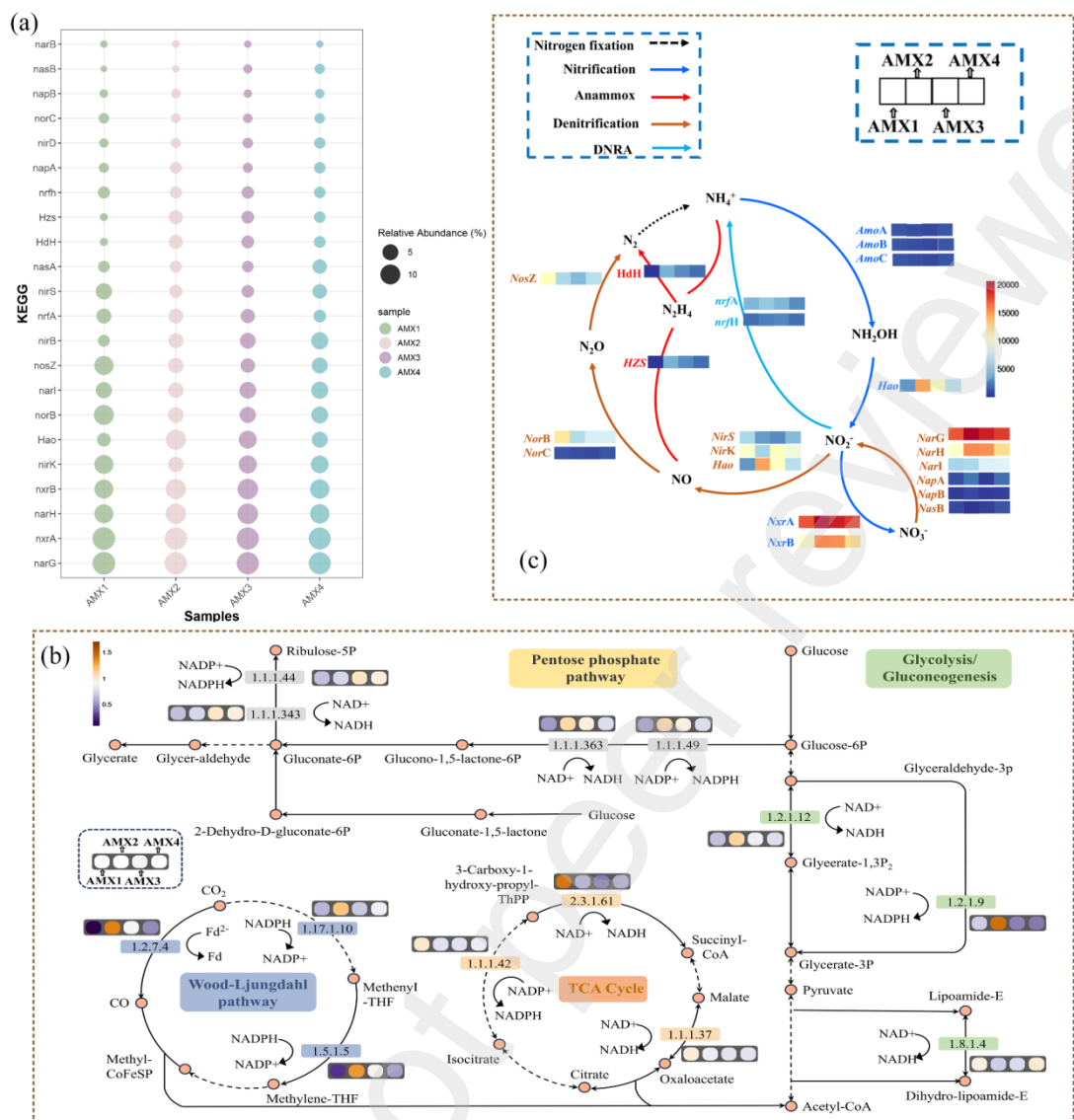


Fig. 5. Metagenomic of the anammox reactor: (a) relative abundance of nitrogen cycle functional genes; (b) nitrogen cycle functional gene mapping; (c) metabolic pathway energy transfer.